



HAL
open science

Ruthenium behavior in the reactor cooling system in case of a PWR severe accident: study of oxidative conditions with stainless steel tube

Marie-Noelle Ohnet, Olivia Leroy, Laurent Cantrel, Teemu Kärkelä

► To cite this version:

Marie-Noelle Ohnet, Olivia Leroy, Laurent Cantrel, Teemu Kärkelä. Ruthenium behavior in the reactor cooling system in case of a PWR severe accident: study of oxidative conditions with stainless steel tube. *Journal of Radioanalytical and Nuclear Chemistry*, 2023, 333, pp.235-251. 10.1007/s10967-023-09230-7. irsn-04324382

HAL Id: irsn-04324382

<https://irsn.hal.science/irsn-04324382v1>

Submitted on 5 Dec 2023

HAL is a multi-disciplinary open access archive for the deposit and dissemination of scientific research documents, whether they are published or not. The documents may come from teaching and research institutions in France or abroad, or from public or private research centers.

L'archive ouverte pluridisciplinaire **HAL**, est destinée au dépôt et à la diffusion de documents scientifiques de niveau recherche, publiés ou non, émanant des établissements d'enseignement et de recherche français ou étrangers, des laboratoires publics ou privés.

Copyright

1
2
3
4
5
6
7
8
9
10
11
12

Title page

Names of authors: Marie-Noelle OHNET¹, Olivia LEROY¹, Laurent CANTREL¹ and Teemu KÄRKELÄ²

Title: Ruthenium behavior in the reactor cooling system in case of a PWR severe accident: study of oxidative conditions with stainless steel tube

Affiliation(s) and address(es) of the author(s):

¹ M.N. Ohnet et al.: Institut de Radioprotection et de Sûreté Nucléaire (IRSN), PSN-RES/SEREX/L2EC, Cadarache, Saint-Paul-Lez-Durance, 13115, France

E-mail address of the corresponding author: marie-noelle.ohnet@irsn.fr

²T. Kärkelä from VTT Technical Research Centre of Finland Ltd (VTT), 02044 VTT, Espoo, Finland

13 **Ruthenium behavior in the RCS in case of a PWR severe accident: study of**
14 **oxidative conditions with stainless steel tube**

15 M.-N. Ohnet¹, O. Leroy¹, L. Cantrel¹ and T. Kärkelä²

16 1: Institut de Radioprotection et de Sûreté Nucléaire (IRSN), PSN-
17 RES/SEREX/L2EC, BP 3, 13115 Saint-Paul-Lez-Durance Cedex, France
18 marie-noelle.ohnet@irsn.fr

19 2: VTT Technical Research Centre of Finland Ltd (VTT), 02044 VTT, Espoo, Finland

20 **Abstract**

21 In the research field on severe accidents in Nuclear Power Plant, a specific scenario correspond
22 to accident with oxidative conditions for which damaged fuel can be highly oxidised with
23 significant releases of ruthenium oxides. Ruthenium chemistry is complex, and the current
24 knowledge has to be deepened to better assess ruthenium Source Term with potential
25 radioactive releases to the environment as volatile ruthenium tetroxide. In this work,
26 experimental studies are focused on ruthenium behaviour along a stainless-steel thermal
27 gradient tube, with maximum temperature of 1200°C, simulating the reactor cooling system in
28 oxidizing conditions with mainly steam/air gas mixtures. Results showed that few % of
29 ruthenium oxides (< 10% with SS tube) can reach low temperature, representative of
30 containment temperature, even with low oxygen content in the carrier gas. The ruthenium
31 revaporization process from the Ru deposits along the tube on mid-term was studied. Influence
32 of carrier gas composition (steam %), flow rate and NO_x feed are discussed.

33 **Keywords** Source term, Severe Accident, Ruthenium transport, Reactor Cooling System, NO₂

34
35 **Introduction**

36 During a hypothetical severe accident (SA) with a core melt down and under oxidizing
37 conditions in a Nuclear Power Plant (NPP), ruthenium may be released from the nuclear fuel
38 and partially transported as gaseous ruthenium oxides to the reactor containment building.
39 Ruthenium is of particular interest because of its high radiotoxicity and its ability to form
40 volatile oxides. It can contribute significantly to radiological consequences on the short and
41 mid-terms due to its two isotopes ¹⁰³Ru and ¹⁰⁶Ru, if released in significant amount to the
42 environment [1]. A previous OECD project, called STEM (Source Term Evaluation and
43 Mitigation) operated by IRSN, investigated the Study of the TrAnsport of RuThenium in the
44 primary circuit (START) [2]. The objective was to provide experimental data to better
45 understand the phenomena leading to gaseous ruthenium release at the break of the reactor
46 cooling system (RCS) [3]. The main objective was to build a first experimental database to
47 guide ruthenium modelling improvements and thus later be able to refine the evaluation of
48 source-term for a SA occurring on a pressurized water reactor (PWR), and to reduce
49 uncertainties on specific phenomena related to the physical-chemistry of one major fission
50 products ruthenium. This experimental project has provided new insights concerning the Ru

51 transport/chemical behaviour in the RCS, focused on medium- and long-term releases during a
52 severe NPP accident.

53 During the START experiments, two phases were studied, a first direct phase called
54 vaporization phase in which Ru was generated from a crucible at 1200°C and a second phase,
55 called revaporization phase, performed without any source of Ru but in presence of Ru deposits
56 along the thermal gradient tube (TGT). The major experimental data measured were amount
57 and identification of Ru species (gaseous and condensed forms) transported at the “cold leg
58 break”, amount of Ru deposit along the TGT as a function of the experimental conditions and
59 amount of the Ru transported during the revaporization phase from the deposits. The purpose
60 was to supply a parametric study to better understand the effect of each single parameter. The
61 first phase of the program gave information on the key parameters impacting the transport
62 kinetics, the partition between gaseous RuO₄ and particles of RuO₂ at low temperature and the
63 extent of the revaporization process of deposited species [3], most of the tests were performed
64 with a glass tube to ensure a better mass balance and exclude/limit possible surface interactions.
65 In START program, with an abrupt thermal profile, steam in excess and a pre-oxidized stainless
66 steel (SS) tube, it was shown that the total Ru transported downstream the TGT led up a
67 maximum of 4.5% of the Ru mass vaporized, mainly under gaseous form. This work showed
68 that the precise steam influence could not be clearly determined for the two phases (direct
69 vaporization and revaporization) and needs additional tests.

70 To complete this first project, complementary tests based on ruthenium revaporization
71 process with representative oxidative conditions (including atmospheric radiolysis simulants)
72 have been performed in the frame of the follow-up OECD STEM2 project (2016 to 2019) [4].
73 In START2, role of oxidative agents and surface state with SS transport tube were examined
74 on ruthenium tetroxide (RuO₄) formation and stability. This paper summarises the main
75 outcomes.

76 First, the revaporization phase required more investigation and an improvement of the test
77 protocol was carried out in START2 with longer duration tests.

78 Second, nitrogen oxides are of special interest regarding ruthenium chemistry. RuO₄ is
79 known for its ability to form different nitroso and nitrosyl compounds after reacting with nitric
80 acid, NO₂ or NO gases [5-7]. RuO₄ can also be trapped into the water phase after reacting with
81 NO₂ or NO gases [8]. Estimation of the amount of NO_x in the containment atmosphere predicts
82 that representative concentrations of NO₂ and N₂O will be a few tens of ppm at most depending
83 on e.g. temperature, dose, gas composition [9, 10].

84 Third, the tests were carried out with a pre-oxidized stainless steel thermal gradient tube to
85 include the potential surface effect (covering a better representativeness of the surface
86 deposition).

87 In the present article we address the influence of steam, gaseous flow rate and NO_x feed
88 on the Ru transport at the TGT outlet, after consecutive vaporization and revaporization phases,
89 for ten relevant experiments.

90

91 **Experimental**

92 The experimental set-up and the test protocol were described in a previous article [3]. For
93 these new experiments, details are provided hereafter.

94 **Reagents**

95 The ruthenium dioxide powder (RuO_2 , purity 99.9%) was purchased from Alfa Aesar. The
96 weight percentage of Ru in RuO_2 powder is 75.8% given by the analysis certificate.

97 The source of NO_2 or N_2O gas in air was purchased from Air Liquide® (450 ppm NO_2 or
98 400 ppm N_2O in the source bottle).

99 **Equipment**

100 The START2 facility (Fig. 1) has been designed as an open flow reactor with a controlled TGT.
101 Temperature gradient, reagent concentrations and residence time are representative of an
102 accidental break of the primary circuit of a nuclear reactor, right up to the measurement point
103 (simulating a cold leg break). A gas supply system with a steam generator (SG) is placed at the
104 entrance of the tube and gas mixtures ($\text{H}_2\text{O}/\text{air}$) are introduced at 150°C upstream of the furnace.
105 The two flow rates studied are 1.84 NL/min or 4.65 NL/min (at 0°C , 101.3 kPa). The tube
106 materials representative of RCS surfaces were Inconel alloy 600 for the high temperature zone
107 in the furnace and Stainless Steel 316L from the exit of the furnace to the TGT outlet (Fig. 2).
108 The tube is 1.80 m long and has an internal diameter of 33 mm. The SS tube was pre-oxidized
109 before the test at 800°C with a rich steam mixture (steam = 80 g/h and air = 14.1 g/h), during
110 24h to form representative oxide layers [11].

111 The device comprised a high temperature furnace and ceramic heaters to control the
112 thermal profile. During the first part of the program, two thermal profiles (abrupt and smooth)
113 were studied with the furnace temperature at 1200°C [3]. All the START2 experiments were
114 performed with an abrupt profile ($\sim 27^\circ\text{C}/\text{cm}$) favoring the gaseous transport at the outlet in
115 accordance with the results obtained previously [3]. In the SS-316L part, the measurement of
116 fluid temperatures between the position at 0.45 m from the crucible and the exit of the device
117 (middle of gas flow, with a step of 5 cm) was performed by six thermocouples during all the
118 duration of the test (Fig. 3). With a tube (0.70-0.75 m long between the crucible and the outlet)
119 and a furnace reference temperature at 1200°C , the fluid temperature at the exit flange of the
120 TGT was around $(290 \pm 20)^\circ\text{C}$ and the residence time from crucible to exit tube ~ 5 seconds
121 with a total flow rate at 1.84 NL/min. With a higher flow rate at 4.64 NL/min (x 2.5), the fluid
122 outlet temperature was around $(410 \pm 30)^\circ\text{C}$ and the residence time decreased to 2 seconds.

123 The test bench was instrumented to allow continuous measurements and control the
124 thermal-hydraulic parameters such as pressure, carrier gas flow rates, wall and fluid
125 temperatures.

126 The NO/NO_2 measurements were performed with a PORTASENS II portable gas leak
127 detector (precision of ± 0.1 ppm for the 10-200 ppm NO_2 range and precision of ± 1 ppm for
128 the 40-500 ppm NO range, with a response time of about 40 sec.). A G200 analyzer dedicated
129 to measure N_2O gas was also used (precision of $\pm 2\%$ for the 0-1000 ppm, with a response time
130 of about 40 sec).

131 **Method**

132 The START2 test protocol (thermal-hydraulic sequence) was adjusted to get a total
133 consumption of the reagent in the first two hours of the experiment. The objective was to
134 conduct the vaporization and revaporization phases without interruption of the furnace heating
135 and of the gas mixture injection in the tube during the night. The goal was reached with reducing
136 the amount of Ru in the crucible (about 10 times less) and using a bigger first liquid trap of

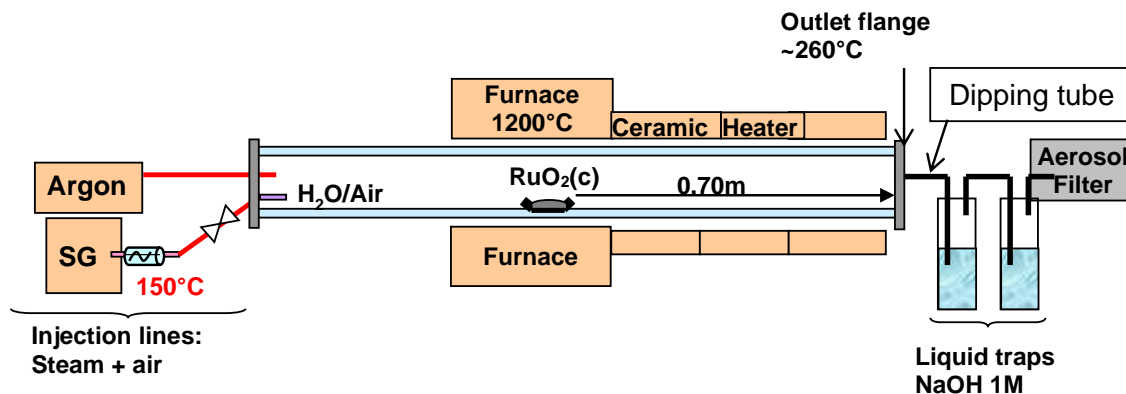
137 1.5 L (Fig. 2). So, this new protocol is more reliable without any disturbing during the long test
138 and results are more confident.

139 The source of Ru, call later “crucible” vaporized Ru mass (i.i.), was previously determined
140 in START project at 1200 °C by mass difference before and after the test. In START2 test
141 protocol, at the end of a long duration test, the crucible was empty. So, the Ru vaporization rate
142 from the crucible obtained in START with 1.84 NL/min were used to determine the duration to
143 consume the entire RuO₂ reagent in the crucible with the gaseous mixture used in the START2
144 tests. With a total flow rate of 4.65 NL/min, complementary experiments with SS tube, a short
145 duration of 1 hour and 300 mg of reagent (anhydrous RuO₂) were performed to determine the
146 Ru vaporization rate from the crucible at 1200 °C with 1%-99%_w and 67%-33%_w of H₂O-air
147 gaseous mixtures. For each test, a mass of 100 mg (flow rate of 1.84 NL/min) or 200 mg (with
148 4.65 NL/min) of anhydrous RuO₂ powder in the alumina crucible was weighted and placed in
149 the furnace the day before the test. This mass allowed a crucible empty at the end of the test.
150 The furnace was heated up to high temperature (1200 °C) under argon, due to low vapor
151 pressure of RuO₂ an infima/negligible amount of RuO₂ is vaporized. When the device was
152 thermally stable, the argon flow was replaced by the oxidizing gaseous mixture (H₂O/air) during
153 20 h for long tests and 6 h or 7 h with NO_x feed. For the conditions with higher flow rate and
154 without NO_x feed, it was not necessary to extend the test duration to second day. The total flow
155 rate (laminar flow) was the same in a set of tests to have a similar residence time for a given
156 temperature profile allowing comparison between tests. At the end of the test, during the set-up
157 cooling down, a low argon flow rate was used to sweep the tube.

158 Separation and quantification of gaseous and condensed (aerosols) ruthenium species was
159 achieved by trapping them into two liquid traps containing NaOH (1M) mounted in series and
160 on an aerosol filter (quartz fiber) located downstream of the liquid traps to avoid parasitic
161 trapping of gaseous Ru. The first liquid trap was cooled down (around 5 °C) to increase the
162 gaseous trapping, with a good efficiency whereas no gaseous Ru is detected in the second liquid
163 trap. For test with steam in excess, the temperature in the first liquid trap increased to 11 °C
164 together with the liquid volume increase. Kinetics evolution of Ru transported at the outlet
165 along the test was followed by sampling regularly the liquid trap solution.

166 For tests performed with NO₂ feed with 1.84 NL/min, it was decided to inject NO₂ gas at
167 the furnace exit, after the high temperature zone, to avoid possible thermal decomposition of
168 NO₂. Therefore, the flow rate over the crucible was 1.64 NL/min completed by 0.2 NL/min of
169 NO₂ feed injected at the exit of the furnace (about 930 °C). In our conditions of gas dilution
170 (flow rate of the NO_x line adapted), we injected about 50 ppm of NO₂ or 40 ppm of N₂O in the
171 tube, respectively. A test like the test with dry air and NO₂ feed at the exit of the furnace was
172 repeated with NO₂ feed at the entry of the TGT. No significant influence was observed on the
173 Ru amount transported at the outlet. Based on previous literature works [12, 13], it was assumed
174 that the low concentration of NO₂ did not have a significant effect on the Ru vaporization from
175 the crucible. So, for tests performed with the higher flow rate, the NO_x feed was done at the
176 entry of the TGT with the flow rate over the crucible of 4.15 NL/min completed by 0.5 NL/min
177 of NO₂ feed (50 ppm).

178



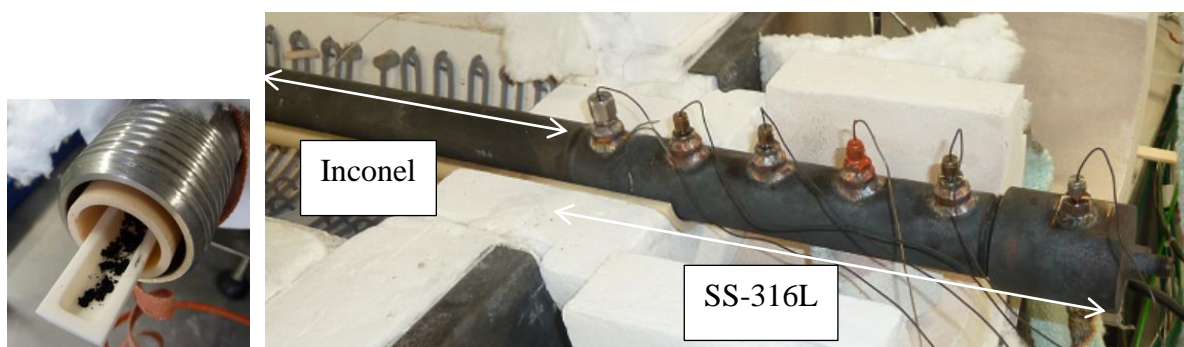
179
180
181

Fig. 1 Scheme of the START2 facility [3].



182
183
184
185

Fig. 2 START2 test facility (left) and RuO₄ dissolved in alkaline solution with the higher liquid trap – steam conditions (right)



186
187
188
189

Fig. 3 Crucible of RuO₂ powder at the entrance of the SS tube (left) and exit part of the pre-oxidized SS tube with fluid thermocouples, without final insulation

190 **Experimental matrix**

191 The matrix composed of 10 tests covers influence of gas compositions, flow rates and test
192 duration. The gas composition H₂O-air is reported in Table 1, with some tests with NO_x feed
193 (NO₂ and N₂O). The reference flow rate is fixed to 1.84 NL/min with variation with a factor x
194 2.5. Test 1 was the reference case with dry air condition (0%-100%_w), an abrupt thermal profile
195 and SS tube. Tests 2 and 3 focused on the effect of the steam-air proportion (60%-40%_w and
196 85%-15%_w). Tests 4 and 5 were dedicated to NO₂ influence with dry air and steam-air mixture
197 conditions respectively. The next tests (6 to 10) were focused on the increase of the flow rate
198 and the NO₂ feed to observe any influence of shorter residence time and Ru concentration.
199 Finally, the last test, numbered 10, was performed with a N₂O feed. With 1.84 NL/min, the
200 composition of the carrier gas mixture (60%-40%_w) was 62.5 g/h for steam mass flow rate and
201 41.8 g/h for air mass flow rate, and 80.0 g/h for steam and 14.1 g/h for air for (85%-15%_w).
202 With 4.65 NL/min, the reference test (6) was performed with (1%-99%_w), 4.1 g/h for steam
203 mass flow rate and 352.8 g/h for air mass flow rate. The composition of the carrier gas mixture
204 (67%-33%_w) was 171.0 g/h for steam and 83.6 g/h for air.

205

206

207 **Table 1** Experimental parameters of START2 tests (316L SS oxidized, furnace temperature
208 1200°C and abrupt thermal profile, RuO₂ source).

Test	Carrier gas H ₂ O-air (% _w weight proportion), NO _x feed	Flow rate (NL/min)	Test duration (min)	Vaporization duration (min), ± 10 min
1	0-100 (ref)			52
2	60-40	1.84	1170	87
3	85-15			67
4*	0-100, NO ₂ (50 ppm)		420	52
5*	52-48, NO ₂ (50 ppm)			87
6	1-99 (ref)		390	94
7	67-33	4.65		170
8	1-99, NO ₂ (50 ppm)		91	
9	67-33, NO ₂ (50 ppm)		360	186
10	67-33, N ₂ O (40 ppm)			169

209 *: For tests 4 and 5, the flow rate over the crucible was 1.64 NL/min (52%-48%_w H₂O/air) completed
210 with 0.2 NL/min of NO₂ feed (at about 930 °C) injected at the exit of the furnace. So, total flow rate of
211 1.84 NL/min with (60-40) mixture for test 5.

212

213 Ru analysis

214 Despite a major part of the Ru released was deposited in the TGT, a significant part was
215 transported to the tube outlet under gaseous and aerosol forms. So, the ruthenium released from
216 the crucible was found on the dipping tube (DT) of the first liquid trap (deposited Ru), in the
217 trapping solution (gaseous and aerosol particles) and on the ultimate filter of the device
218 (assumed to be only aerosol particles). The Ru measurements for these different places
219 (essentially performed with ICP-AES) are detailed in [3]. To determine the Ru amount in
220 gaseous phase and in aerosols particles, liquid trap solutions were centrifuged and filtered at
221 the end of the experiment. The final solution filtered was analyzed by ICP-AES (gaseous RuO₄
222 dissolved in NaOH) and the filter with aerosol particles was dissolved by alkaline fusion and
223 analyzed by ICP-AES.

224 Contrary to the tests performed with quartz tube in the first part of the program, the Ru
225 deposit profile along the SS tube could not be measured. This material does not allow dissolving
226 the deposits by alkaline fusion. So, the amount of Ru deposits is determined by the difference

227 between the Ru amount vaporized from the crucible and the total Ru amount transported at the
228 tube outlet (gas + aerosol particles + Ru deposit on dipping tube of liquid trap).

229 For each test, the partition of Ru transported during the vaporization and revaporization phases,
230 respectively, is determined. There is no gas / aerosol particle differentiation in this partition as
231 it is carried out from the total Ru data (gas and aerosol particles) transported in the trapping
232 solution (1st liquid trap). The amounts transported in each phase are expressed in percent of the
233 vaporized Ru mass (i.i.). Concerning the revaporization contribution, the percentage
234 transported is also expressed in term of the i.i. and not of the actually revaporizable amount
235 deposited into the tube because it is not possible to determine it with accuracy.

236 First, the time required for the total consumption of the reagent in the crucible is estimated
237 (vaporization phase duration) with the vaporization kinetics (in mg / min) of the tests carried
238 out and the initial mass of Ru in the crucible. Then, according to the graph "Evolution of the
239 Ru amount in the first trap", the transport kinetics (in $\mu\text{g} / \text{min}$) of the ruthenium transported is
240 established. The duration of the vaporization phase is used in the transport equation to know
241 the Ru amount transported only during this phase.

242 For the revaporization phase, two cases may occur:

243 - Either the revaporization is finished before the end of the test, characterized graphically by a
244 stabilization of the Ru amount transported in the liquid trap;

245 - Or the revaporization is not completed at the end of the test, characterized graphically by an
246 increase in the amount trapped in the liquid trap.

247 In the first case, the beginning of the stabilization (end of transport of Ru) is determined
248 graphically. The real revaporization duration is the difference between the end of the
249 vaporization phase and the beginning of the stabilization. The Ru amount transported during
250 this phase is the difference between the Ru amount transported at the end of the test and the
251 value determined at the end of the vaporization phase.

252 In the second case, it is not possible to estimate the duration of the revaporization phase
253 while it is not achieved. The Ru amount transported during the revaporization is estimated in
254 the same way (final amount minus amount at the end of vaporization). The calculated
255 percentage will therefore be a minimum value of the contribution of the revaporization.

256 This partition is based on the graphical estimation of the Ru (gas and aerosol particles) and
257 the average kinetics. So, a difference could be observed between the sum of the percentages
258 attributed to each phase and the percentage of final transported Ru which considers the gas /
259 aerosol particle partition.

260 According to the feedback of the previous program, RuO_4 trapped in NaOH 1 M is not
261 stable in time and tends to precipitate as insoluble RuO_2 . Thus, the last sample of day 1 is
262 analyzed and then stored at 4°C (temperature like that of the liquid trap 1). This same sample
263 is analyzed again the next day to estimate the "loss" linked to the instability during the night.
264 When the loss is greater than 10% (uncertainty criterion), the values obtained during the ICP
265 analysis are corrected by the percentage previously determined.

266

267 **RESULTS AND DISCUSSION**

268 The following sections are dedicated to the comparison of the test results according to the
269 studied parameters to evaluate the potential influence of each one. All the results obtained in
270 the START2 test matrix are summarised in **Table 4**.

271

272 **Ru mass vaporization kinetics**

273 The Ru vaporization rate from the crucible at 1200°C and a flow rate of 1.84 NL/min with
274 quartz and SS tube was determined previously [3]. The values are detailed in **Table 2**. The dry
275 air condition was the most favorable condition for Ru vaporization. The release of Ru from the
276 crucible at 1200°C in a SS tube with 1.84 NL/min flow rate is ranging from 0.8 to 1.5 mg/min.
277 With a higher flow rate at 1200°C, dedicated tests were performed in START2 (**Table 2**). The
278 modification of geometry between the SS and Q tube induced an increase of the kinetics for the
279 SS tube (*factor 1.2*). It is probably due to the reduction of the internal diameter in the hot zone
280 (from 30 to 23 mm [3]) and the height of the crucible containing the Ru powder which was
281 decreased by half (compared to START experiments with a quartz tube) thereby improving the
282 surface air/reagent exchange in the SS tube configuration. It was highlighted that the crucible
283 used in START2 tests had a limiting interface effect on the Ru release behavior, with a
284 maximum value close to 1.8 mg/min compared to 6.1 mg/min with a flow rate of 5 NL/min in
285 VTT-NKS studies [13]. The vaporization kinetics for 85%/15%_w H₂O/Air gaseous mixture with
286 SS tube and 1.84 NL/min was not experimentally determined but was estimated from the
287 average of the quartz tube and 85%/15% mixture condition tests ($0.67 \times 1.2 = 0.8$ mg Ru/min).

288 Previously [3], it was demonstrated that the release rate of Ru decreases with the oxygen
289 partial pressure. The same tendency is observed with 4.65 NL/min as expected.

290 Therefore, the durations of vaporization phase estimated from the total Ru consumption of
291 RuO₂ reagent for each test are presented in **Table 3**. The duration estimated for test 5 was
292 87 min, as test 2. This value is probably slightly over-estimated because the flow rate over the
293 crucible was smaller (1.64 NL/min) than for test 2 (1.84 NL/min). For test 4 with dry air, this
294 duration was estimated to about 50 min, like test 1.

295 To conclude, the flow rate, the crucible geometry with gaseous flow rate leaching the
296 reagent powder surface or not, and the gaseous composition (O₂ %) are important parameters
297 for the Ru vaporization rate at a given temperature.

298

299 **Table 2** Experimental values of the Ru vaporization kinetics for different gaseous mixture
300 studied with SS tube.

Gaseous mixture	Average kinetics (mg/min)	Kinetics (mg/min)
H ₂ O-Air (% _w)	1.84 NL/min	4.65 NL/min
0-100	1.50 ± 0.02	/
1-99		1.75 ± 0.02
60-40	0.93 ± 0.02	/
67-33	/	0.90 ± 0.02
85-15	0.80 ± 0.13 (estimated)	/

301

302 **Table 3** Vaporization kinetics and estimated duration for the total Ru consumption.

Test	Gaseous mixture H ₂ O-air (% _w)	Kinetics (mg/min)	Initial mass of reagent RuO ₂ (mg)	Ru mass vaporized (to express all results as % i.i.)	Duration for the vaporization phase (min)
1	0-100	1.50	104	79	52
2	60-40	0.93	106	81	87
3	85-15	0.80	71	54	67
4	0-100	1.50	104	79	52
5	52-48	0.91	105	79	87
6, 8	1-99	1.75	218, 210	165, 159	~92
7, 9, 10	67-33	0.90	201, 201 221	153, 152, 168	169-186

303

304 **Total Ruthenium transported in vaporization and revaporization phases**

305 The results are summarized in **Table 4** where the Ru amounts transported at the TGT outlet
306 (gaseous and total with aerosol particle fraction and dipping tube deposits) are presented with

307 the repartition of Ru coming from vaporization and revaporization phases. All the data are
 308 expressed as % of “crucible” vaporized Ru mass. The results of the long tests 1 and 2 (1770 min)
 309 have been expressed at the end of the first day of experiment (420 min) to be compared easily
 310 with others tests at similar duration.

311 All the tests performed with SS tube and an abrupt profile conducted to Ru transport at the
 312 tube outlet. For tests with the lower flow rate and without NO_x feed, the total Ru transported
 313 represents from 4% to 8% of “crucible” vaporized Ru mass while it represents about three times
 314 more for the higher flow rate (13% to 18.5%). When the revaporization phenomena are not
 315 finished at the end of the experiments (tests 3, 7 and 10), the values obtained are minimal values.

316

317 **Table 4** Results at tube outlet in % of “crucible” vaporized Ru mass (i.i.), for long time duration
 318 (tests 1, 2 and 3) and after the first day of experiment (other tests).

Test	Test duration (min)	RuO ₄ (gaseous) ^a (%)	Ru Total ^a with DT deposit (%)	Ru during Vaporization ^b (%)	Ru during Revaporization ^b (%)
1	1770	6.6	7.9	1.3	4.9
	420	4.5	5.2	1.3	2.9
2	1770	3.4	6.2	0.4	3.3
	420	0.9	2.1	0.4	0.8
3	1770	3.1	4.3 ^c	0.6	2.5 ^c
4	420	1.0	3.5	1.3	1.6
5	420	1.0	2.9	0.4	0.5
6	390	11.4	18.5	6.5	5.3
7	390	7.7	13.5 ^c	6.4	1.9 ^c
8	390	10.1	13.1	7.0	5.2
9	360	1.85	10.5	2.4	0.7
10	360	5.1	13.6 ^c	2.4	3.0 ^c

319 ^a: Uncertainties for Ru amount transported at the outlet: ± 0.2% for tests 4 and 5, ± 0.3% for
 320 tests 3 and 7, ± 0.4% for test 2, ± 0.7% for test 1, ± 0.8% for test 9, ± 1.3% for tests 6, 7 and 10.

321 ^b: Gas and aerosol particles in 1st liquid trap without Ru deposit in the DT.

322 °: The revaporization phase was not finished at the end of tests 3, 7 and 10.

323

324 **Gaseous composition effect**

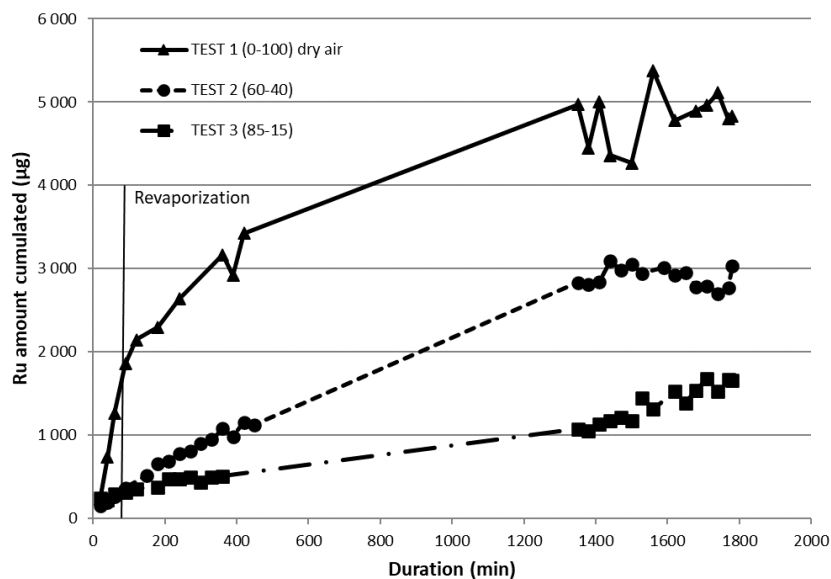
325 The START2 tests allowed completing information on the effect of gaseous composition with
 326 pre-oxidized SS tube and on revaporization process. With a furnace temperature at 1200°C and
 327 abrupt profile, a flow rate at 1.84 NL/min, kinetics of Ru transport at the tube outlet were linear
 328 and similar for the two phases: vaporization and revaporization in condition mixture with steam
 329 (Fig. 4). Kinetics of Ru transport at tube outlet was equal to 2 µg/min and 0.67 µg/min for tests
 330 2 and 3, respectively. For the test with dry air, the kinetics was higher than for the two other
 331 tests performed with steam mixtures, equal to 23 µg/min to 90 min (vaporization phase) and
 332 4 µg/min in the range 90-420 min with end of revaporization around 800 min. Revaporization
 333 process could take place during the vaporization phase but kinetics of revaporization is lower
 334 than kinetics of vaporization. The Ru transport was completed before the end of the test (~1400
 335 min) for 2 tests (0%-100%_w and 60%-40%_w) while it was not reached for the 85%-15%_w test
 336 (~1800 min).

337 The mixture H₂O-air composition influences the total Ru amount transported at the TGT
 338 outlet. Air content promotes the Ru amount transported at the outlet (Fig. 5, **Table 4**).

339 In long duration test 2 (60%-40%_w), the Ru plateau revaporization was reached with a final
 340 gaseous value of 3.4 % i.i., value higher than that observed in previous tests [3] but for shorter
 341 duration without plateau.

342 To conclude, the maximum gaseous Ru amount measured of 6.6% of “crucible” vaporized
 343 Ru mass was obtained with dry air condition (including both vaporization and revaporization
 344 phases). With steam in large excess in the gaseous mixture (85%-15%_w), which are the most
 345 representative conditions of a hypothetical severe accident occurring on a PWR, this value was
 346 about half (3.1 % i.i.), in the same order of magnitude with (60%-40%_w) mixture. A major part
 347 of the Ru source term came from the revaporization process on the “long term” (Fig. 5).

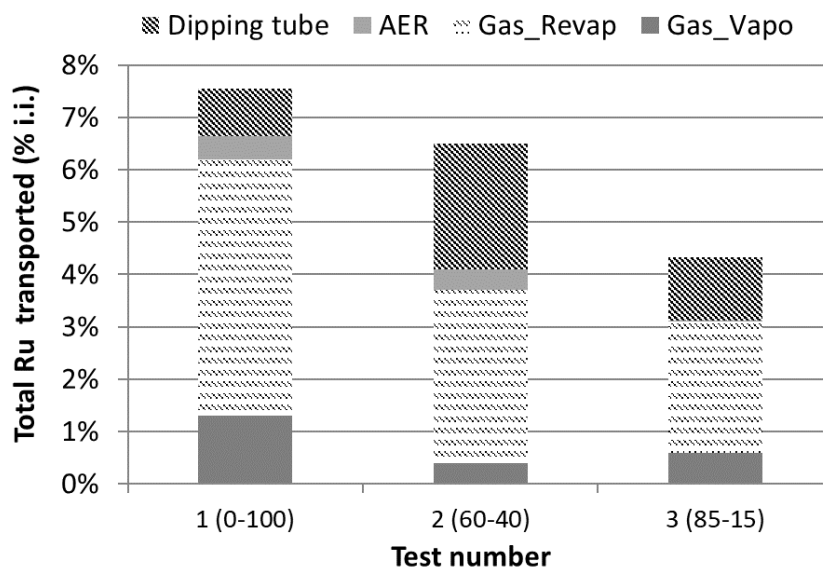
348



349

350 Fig. 4 Evolution of the Ru amount in the first liquid trap as a function of the H₂O-air gaseous mixture

351



352

353 Fig. 5 Ru gaseous partition from vaporization and revaporization, aerosols (AER) and Ru deposited
354 into the Dipping Tube at the end of the tests 1, 2 and 3 (% i.i.) with a pre-oxidized SS tube

355

356 Recent NKS (Nordic nuclear safety research) studies on transport of ruthenium in thermal
357 gradient tube had been performed by I. Kajan *et al.* [13] and previously by T. Kärkelä [14]. The
358 experiments were realized with a flow rate of 5 NL/min (TGT internal diameter of 22 mm) and
359 the results obtained are quite different from those of START2 with 1.84 NL/min, with mostly
360 aerosols at the outlet except with NO₂ which favors the gaseous phase. So, we have performed
361 some START2 tests with a higher flow rate to be closer to NKS-VTT condition and allowing a
362 better comparison.

363

364 Flow rate effect

365 Two complementary tests without NO_x (tests 6 and 7) were performed at 1200°C to evaluate
366 the impact of a higher carrier gas flow rate (factor of 2.5) on the Ru transport at the tube outlet
367 (Table 4).

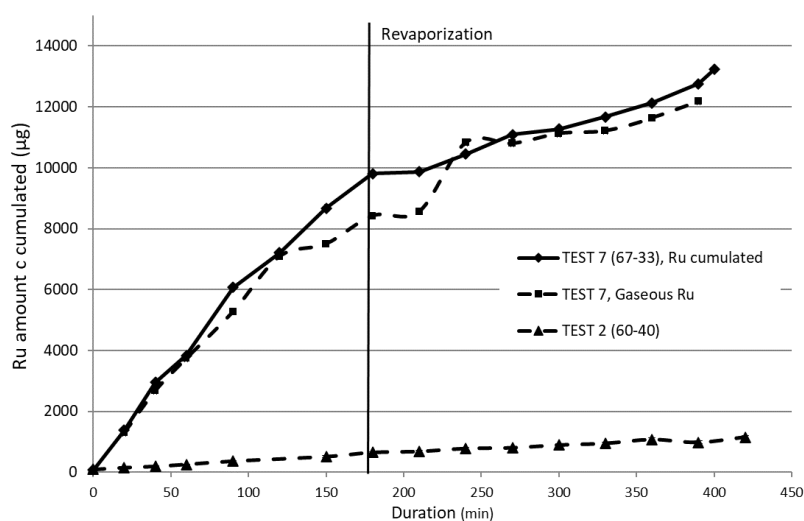
368 With dry air (test 6), kinetics of Ru transported was linear for the two phases with about
369 117 µg/min for the vaporization phase (0-90 min) and 25 µg/min for the revaporization phase
370 (105-270 min), to reach a plateau (300-420 min). With steam condition (test 7), kinetics of Ru
371 transported was linear for the two phases with about 54 µg/min for the vaporization phase (0-
372 170 min) and 16 µg/min for the revaporization phase (210-390 min). With the two mixture
373 compositions, there is a break of the slope between vaporization and revaporization phases (Fig.
374 6). The contribution of gaseous Ru amount transported to the outlet is similar during the
375 vaporization and the revaporization process (about 6% i.i.) with dry air. While with steam
376 mixture, the revaporization is significantly decreased (~2%) but the revaporization was not
377 finished at the end of the test.

378 With a pre-oxidized SS tube, a furnace temperature of 1200°C, an abrupt thermal profile
 379 and a flow rate of 4.65 NL/min, most of the vaporized Ru was deposited in the thermal gradient
 380 tube (> 80% i.i.) whatever the carrier gas composition. With a steam rich mixture (67%_w), after
 381 6h30 of experiment, the total Ru amount (gaseous and aerosol particles) transported to the tube
 382 outlet represented up to 13.5% i.i., with 7.7% i.i. under gaseous form (Fig. 7). This value is
 383 higher by a factor of about 7 versus the test with 1.84 NL/min on the total transported Ru (1.9%
 384 i.i. in test 2 after 6h30) and on the gaseous transported Ru (0.9%). With almost dry air (1%
 385 H₂O), the total Ru amount transported to the tube outlet represented up to 18.5% i.i., the major
 386 part being in gaseous form (11.4% i.i. without DT deposits). This value is higher by a factor of
 387 2.5 versus the test with 1.84 NL/min on the gaseous transported Ru (4.5% i.i. in test 1 after 7h).
 388 The steam condition decreased the total Ru transported at the outlet, similarly to the results
 389 observed with the lower flow rate (Fig. 5).

390 With the higher flow rate, the fluid temperature at the exit flange was hotter (+ 70°C for
 391 test 7) and the Ru deposit in the DT was more important (x10) because of a stronger thermal
 392 gradient in the pipe of the first liquid trap.

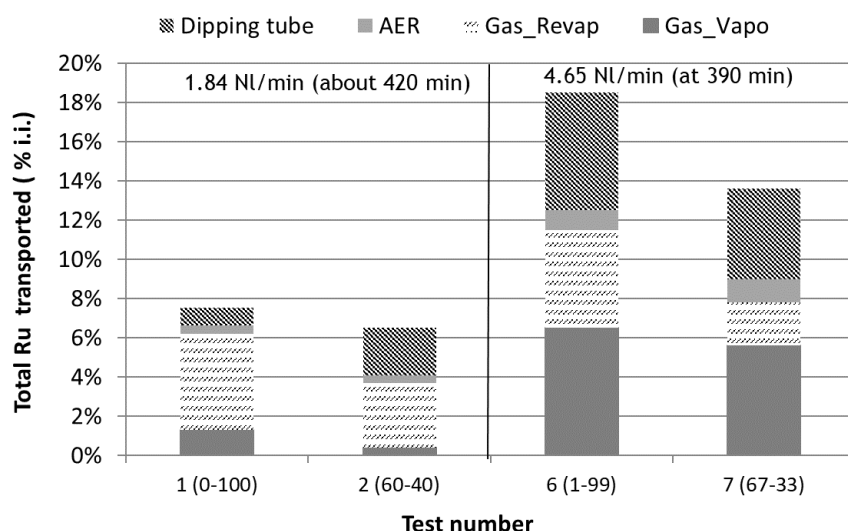
393 The main conclusion is that there is a positive impact of the flow rate increase on the total
 394 Ru amount transported at the outlet, principally on the gaseous form (Fig. 7). Nevertheless, the
 395 revaporization phase was less efficient and shorter, leading to smaller formation of gaseous
 396 ruthenium on the long term.

397



398
 399 Fig. 6 Evolution of the gaseous Ru (dotted line) and the raw Ru mass in the first liquid trap of test 7, under
 400 (67%-33%) H₂O-air mixture and a higher flow rate (4.65 NL/min) and of test 2 under (60%-40%) H₂O-air
 401 mixture

402



403

404 Fig. 7 Ru gas, Ru aerosol particles AER (from first liquid trap and filter) and Ru deposits in the dipping
 405 tube at about 420 min (% i.i.). The Ru transport was not finished at the end of test 7

406

407 **NO_x potential effect**

408 The START2 tests performed with a NO_x (NO₂ or N₂O) feed allowed completing information
 409 on the potential impact of more-oxidizing conditions, like those induced by air radiolysis
 410 products.

411 In our test conditions with 1.84 NL/min, the addition of NO₂ (50 ppm) in the carrier gas
 412 has a weak effect on the Ru transport at the tube outlet whatever the gaseous composition (dry
 413 air or steam in excess in air), as shown in Fig. 8. In presence of NO₂, there is no significant
 414 break of the slope between vaporization and revaporization phases with a similar Ru transport
 415 kinetics (~20 μg/min with dry air and ~2 μg/min with steam, tests 4 and 5 respectively), but the
 416 revaporization phase was less efficient and shorter, leading to smaller formation of volatile
 417 ruthenium. It can be due to RuO₃(g) oxidation by NO₂ (RuO₃(g) + NO₂ ⇌ RuO₄(g) + NO with
 418 ΔG_R^o(1000°C) < 0), leading to less Ru deposits at high temperature. The results obtained with
 419 the NO₂ feed at the furnace exit allow deducing that there is no NO₂ effect on the Ru deposits
 420 at temperature below 900°C in agreement with the thermodynamic view: RuO₂(s) + 2 NO₂ ⇌
 421 RuO₄(g) + 2 NO with ΔG_R^o > 0 for T < 1000 °C. With dry air (test 4), after 1h of experiment,
 422 there was an evolution of the gaseous/aerosol partition with an increase of Ru aerosols amount.
 423 At the end of the test, and for the first time in the START program, some black deposits were
 424 observed on the glass wall of the first liquid trap (estimated at 0.9% i.i.). This observation agrees
 425 well with Igarashi's H. study [8] where the authors concluded that "NO or NO₂ can react with
 426 RuO₄ to form nitro complex of nitrosyl ruthenium Ru(NO)(NO₂)₂(OH).2H₂O which was more
 427 soluble into water and less volatile" and "This transformation was proved by the black deposits
 428 in the glass tube". In the same way, Klein et al. [15] observed that "the gas phase reaction of
 429 RuO₄ and nitrogen oxides formed fewer volatile compounds of Ru".

430 With a flow rate of 4.65 NL/min, a steam rich H₂O/air mixture more representative of
 431 severe accident with oxidizing condition (67/33 %_w H₂O/air mixture, test 9), most of the
 432 vaporized Ru was deposited in the thermal gradient tube (> 80% of "crucible" vaporized Ru
 433 mass, i.i.) as observed without nitrogen dioxide. At the end of the experiment, the total Ru

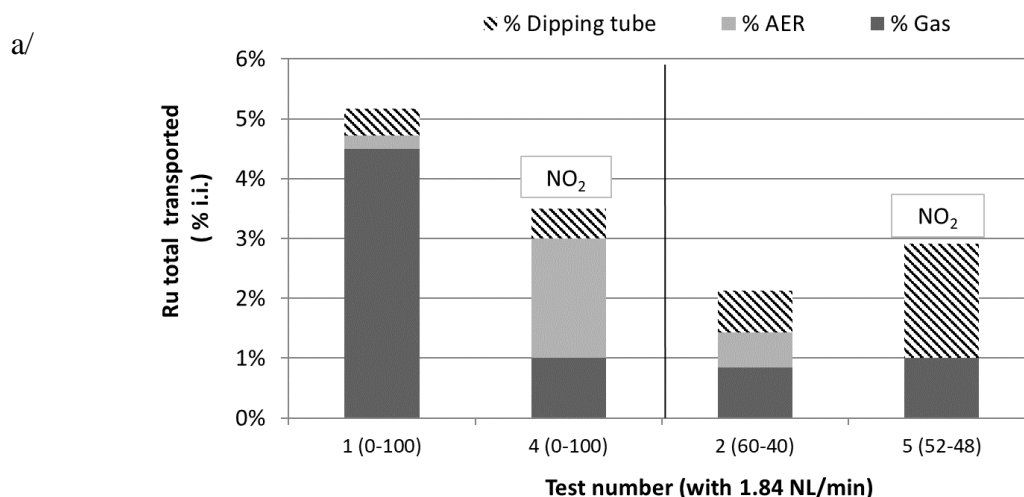
434 amount (gaseous and aerosols) transported to the tube outlet with NO₂ feed represented up to
435 10.5% i.i., in the same order of magnitude than in the reference test without NO₂ (13.5% i.i.,
436 test 7). But the gaseous fraction of volatile ruthenium was significantly lower, 1.8% with NO₂
437 versus 7.7% without NO₂ (Fig. 8). Kinetics of Ru transport was linear for the two phases with
438 about 21 µg/min for the vaporization phase (0-170 min) and 2.5 µg/min for the revaporization
439 phase (210-360 min). Contrary to test 7, the Ru transport was finished at the end of the test 9.
440 So, with NO₂ feed, the Ru transport kinetics are really lower for vaporization and revaporization
441 phases. With almost dry air (1%_w H₂O, test 8), no impact of NO₂ feed (50 ppm) was observed
442 on the gaseous Ru amount transported at the tube outlet (about 10% ii) and on the RuO₄/RuO₂
443 partition, similar to the results obtained with the lower flow rate (1.84 NL/min). Kinetics of Ru
444 transport during the vaporization phase (111 µg/min) is similar to the one observed in test 6
445 (117 µg/min). No effect of NO₂ was observed on the revaporization. Similar to test 6, the
446 contribution of gaseous Ru amount transported to the outlet is similar during the vaporization
447 (6-7 % i.i.) and the revaporization process (5 % i.i.).

448 With steam in excess and the higher flow rate, the total Ru amount (gaseous and aerosols)
449 transported to the tube outlet with N₂O feed represents a maximum value of 13.6% i.i. (test 10),
450 similar to the reference test 7 without NO₂ (13.5% i.i.). But the revaporization phase was not
451 finished at the end of these two tests. Kinetics of Ru transport was linear for the two phases
452 with about 23 µg/min for the vaporization phase (0-170 min) and revaporization phase (210-
453 390 min). This trend is different than in test 7 with respectively 54 µg/min and 16 µg/min.
454 Finally, the contribution of gaseous Ru amount transported to the outlet is similar during the
455 vaporization (2.4 % i.i.) and the revaporization process (3 % i.i.). So, concerning the N₂O feed
456 (test 10), no noticeable effect was observed on the total Ru amount transported at the tube outlet
457 similarly to [12] even if the partition gas/aerosol is a bit different. The gaseous Ru amount was
458 lower, but the Ru deposited into the dipping tube was higher.

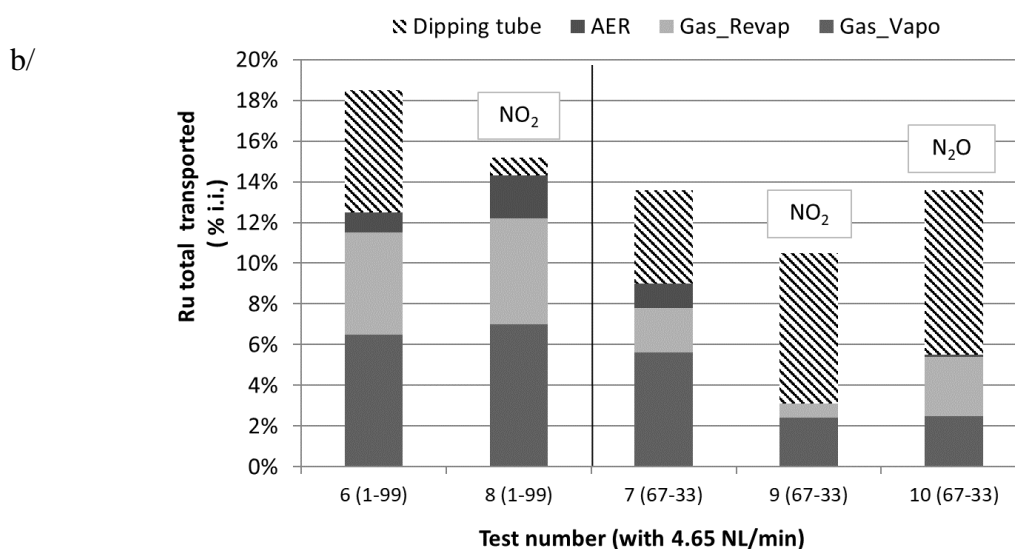
459 Without considering the Ru deposits into the dipping tube of the first liquid trap, the Ru
460 amount transported at the outlet under gaseous form tends to decrease with NO_x feed and steam
461 mixture condition.

462 To conclude, with a pre-oxidized SS tube, a flow rate of 4.65 NL/min, a furnace
463 temperature at 1200 °C, abrupt thermal profile, and a fluid TGT exit temperature at about
464 410 °C, the addition of NO₂ or N₂O tends to slightly decrease the gaseous Ru transport at the
465 tube outlet whatever the carrier gas composition (dry air or steam in excess in air).

466



467



468

469 Fig. 8 : Ru gas, aerosols, and deposits in the dipping tube (% i.i.) at 420 min with 1.84 NL/min (a) and
 470 at 390 min with 4.65 NL/min (b). The Ru transport was not finished for tests 1, 2, 7 and 10

471

472 For revaporization phase, it has been shown [3] that only Ru high temperature deposits (>
 473 900°C) are concerned, temperature where NO₂ was not thermally stable and thus cannot affect
 474 revaporization process.

475

476 **Discussion**

477 **a/ Thermal stability of NO₂**

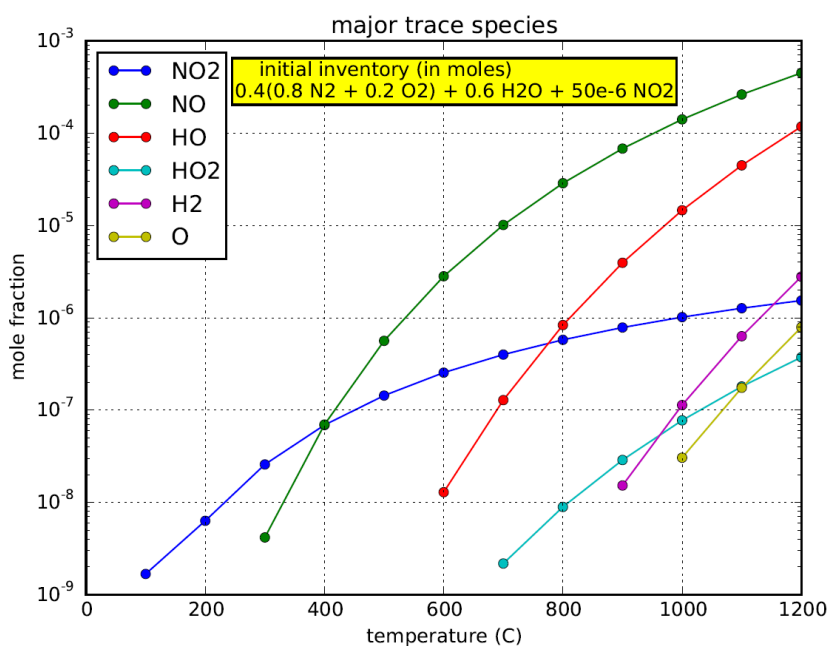
478 We have studied the thermal stability of NO/NO₂, with measurements of NO_x at the exit tube
 479 with NO_x feed at the entry or exit of furnace.

480 The measurements of NO_x/NO at the outlet tube in our thermal-hydraulic conditions (pre-
 481 oxidized SS tube, dry air and 4.65 NL/min) led to a thermal decomposition of NO₂ and N₂O
 482 gas, estimated taken place near 400 °C and 1010 °C, respectively. With NO₂ feed (50 ± 5 ppm),.

483 only NO was measured at the exit (46 ppm) with 800 °C or 500 °C all along the tube. When the
 484 furnace temperature decreased to 370 °C, 55 ppm of NO₂ was measured again at the exit. The
 485 measurements of NO₂ with SS tube before and after the pre-oxidation of the tube (tube without
 486 Ru deposits), and with a quartz tube, showed that there was no effect of the surface state. So,
 487 the thermal decomposition of NO₂ in our conditions was estimated beyond 400 °C, in
 488 accordance with thermodynamic data. N₂O was irreversibly decomposed ($N_2O \rightarrow N_2 + \frac{1}{2} O_2$),
 489 no N₂O and no NO were measured at the outlet tube with furnace at 1200 °C and abrupt profile.
 490 This result agrees with literature [16]. Even if N₂O could exist at high temperature due to kinetic
 491 limitations, it has been shown from ab-initio calculations [17, 18] that the kinetics of the
 492 reactions between ruthenium oxides and nitrogen oxides are low.

493 Thermodynamic equilibrium calculations with a steam/air mixture and 50 ppm of NO₂
 494 show that beyond 400/500°C NO is preponderant with respect to NO₂ which is partially
 495 decomposed as reported in Fig. 9. Even if NO₂ is not stable at elevated temperatures, it could
 496 be continuously formed by air radiolysis induced by the radiation from the fuel or from fission
 497 products deposited onto the RCS walls and thus exist resulting from competitive processes
 498 between formation and destruction pathways according to some kinetic effects. So, it was
 499 decided to inject NO₂ into the START tube at the furnace exit (tests 4 and 5), near 900°C
 500 (corresponding to the Ru deposit zone at high temperature), to limit the decomposition of NO₂
 501 in the furnace zone at 1200°C.

502



503

504

Fig. 9. Thermodynamic calculation with NO₂

505

506 So, with a furnace temperature at 1200°C, an abrupt profile, and a fluid temperature at the exit
 507 flange near 400°C, it seems that NO₂ and N₂O could not reach the crucible zone with Ru and
 508 NO₂ could not be formed again in the part of the tube near the exit flange to react with RuO_x
 509 gaseous form or the small amount of Ru deposits, respectively. Effectively, in START2 tests
 510 performed with a pre-oxidized SS tube, no noticeable increase of the gaseous Ru amount

511 transported at the outlet was observed with NO_x feed (50 ppm) whatever the total flow rate and
 512 the gaseous composition (low or excess of steam amount), **Table 4**.

513 **b/ Consistency with NKS-VTT results**

514 This paragraph details the characteristics of the two experimental set ups (VTT and START2),
 515 as reported in Table 5. VTT's facility is schematically described in [13].

516

517

Table 5 Parameters for the two devices.

Device	VTT	START2 (test 9)
Tube geometry:		
Length from crucible to exit	130 cm	70 cm
Internal diameter	22 mm	32.7 mm (23 mm in the furnace)
Material tube	Alumina + pure SS (316L) (not pre-oxidized)	Inconel 600 + pre-oxidized SS 316L
Alumina Crucible	20 x 2 cm	8 x 0.8 cm
Reagent mass (RuO ₂)	1 g (or 2 g)	200 mg
Furnace temp.(°C), profile	1227 °C, abrupt	1200 °C, abrupt
Temperature at the exit	~40 °C (inner)	~410 °C (fluid)
Flow rate (NL/min)	5 (2.5 + 2.5)	4.65 (4.15 + 0.5) « laminar flow »
NO ₂ feed	Injected to the furnace using an inner tube (through the entry flange), which opening was downstream the crucible location inside the furnace	Injected by the entry flange
H ₂ O-air mixture	2.1x10 ⁴ ppmV H ₂ O (2%mol H ₂ O)	67% _w H ₂ O -33% _w air (77%mol H ₂ O)
Test duration (min)	20 min with NO _x , such as NO ₂ 60 min for other tests	390
Experimental protocol	Oxidative gas injection when 1227 °C was reached (T0)	Oxidative injection after 1h at 1200 °C (T0+1h) with a low argon flow before (5h)

Filter position	before liquid traps (Mitex® 5µm PTFE)	after liquid traps (quartz paper 0.3µm)
-----------------	---------------------------------------	---

518

519 The results of the main tests (gaseous and aerosol particle partitioning) are presented in Fig. 10.

520

521 NKS (Nordic nuclear safety research) study on transport of ruthenium in the primary
 522 circuit [13] concluded that humidity (saturated at room temperature) significantly increased the
 523 Ru transport through the facility, mainly in the form of RuO₂ aerosol (19.8% of Ru released)
 524 compared to dry air condition (8.2%). This trend was not observed with our results, with
 525 principally gaseous phase without particles at the outlet, with the different thermal-hydraulic
 526 conditions from those in VTT facility.

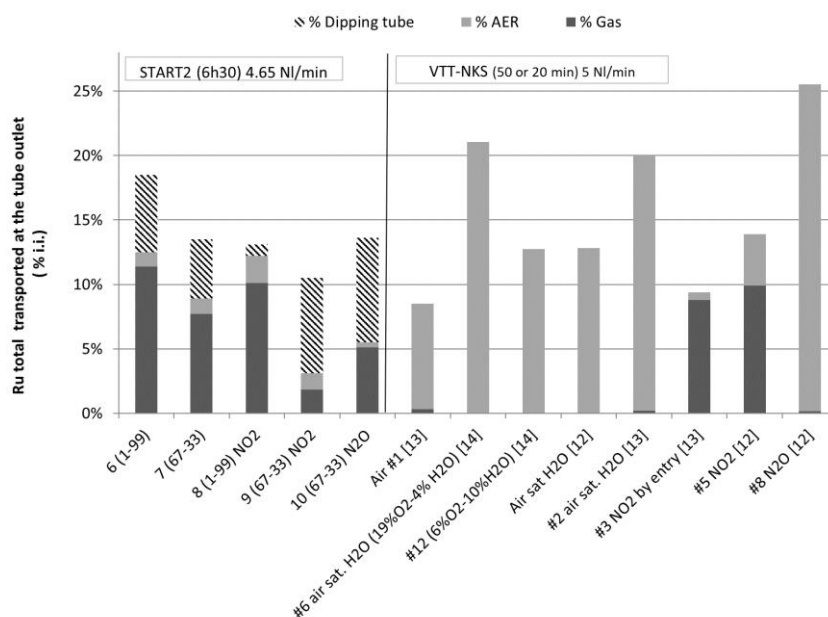
527 If we focus on gas composition effect, Test 7 and VTT test #12 [14] are quite similar in
 528 term of O₂ content (67%H₂O-7%O₂ and 10%H₂O-6%O₂, respectively). If we compared the
 529 total Ru amount transported at the outlet, the results are similar (~13% i.i.). The main difference
 530 is the Ru composition at the TGT outlet with a mix between aerosol and gaseous forms for
 531 IRSN, whereas the aerosol form was largely dominant in the VTT test. The formation of
 532 aerosols can be promoted by a strongest gradient tube in VTT conditions.

533 Test 6 can be compared with VTT test #6 [14] and Kajan test #2 [13], these tests being
 534 performed with a very large proportion of air. The VTT and Kajan's results concerning total
 535 Ru amount transported at the outlet (~20% i.i.) are close to our test 6 result, see **Table 4**. As for
 536 IRSN test 7 with steam, the main difference comes from the nature of the species transported,
 537 mainly in aerosols form at the opposite of IRSN result, it is consistent with that VTT facility
 538 seems to promote nucleation processes (higher source of Ru and lower outlet temperature).

539 I. Kajan *et al.* [12] observed a decrease of the formation and transport of particles
 540 significantly when NO₂ gas (75 ppm) was fed. At the same time, the transport of gaseous
 541 ruthenium increases by about two orders of magnitude (8.8% of Ru released, test #3) compared
 542 to pure air experiment (0.2%, test #2) and total Ru amount transported at the outlet remains
 543 similar. This trend was not observed with START2 conditions; the major species transported
 544 being in gaseous form.

545 With N₂O feed, the results obtained with the two studies (IRSN test 10 and test #8 [12],
 546 Fig. 10) showed the same tendency, with no influence on the Ru transport at the outlet. This
 547 result agrees with the irreversible decomposition temperature estimated near 1000°C. By the
 548 way even if some N₂O persists due to some kinetic limitations, the kinetics of
 549 (RuO₃ + N₂O → RuO₄ + N₂) is very low as shown by Miradji *et al.* [18] with an Arrhenius
 550 energy computed at 106 kJ/mol.

551



552

553 Fig. 10 : Ru amount partition (Gas, Aerosol particles and Ru deposit into the Dipping Tube of the first
 554 liquid trap) in START2 (vaporization and revaporization) and VTT-NKS studies [12-14] with the higher
 555 flow rate

556

557 NO₂ influence differs between VTT and IRSN results. In a first approach, it was supposed
 558 that it could be due to the different flow rates, but the START complementary tests performed
 559 with 4.65 NL/min (tests 8 to 10) do not confirm this assumption even if there is a slight
 560 difference in inner diameter. The residence times are quite close in VTT and IRSN studies (4s
 561 and 2s respectively). Main differences result from the tube geometry, the Ru source mass
 562 flowrate, the gradient profile with the temperature at the exit flange and the tube materials.

563 Firstly, the ratio S/V of VTT set-up (182) is higher than the IRSN's one (Table 5), favoring
 564 the decomposition of gaseous Ru into aerosols by a process occurring on the SS surface, the
 565 first stage being adsorption of RuO₃ and/or RuO₄ on surface before being reduced into RuO₂.

566 Concerning the Ru vaporization rate from the crucible, in VTT-NKS studies [12-14], at
 567 1227 °C with a low amount of steam and a flow rate of 5 NL/min, a Ru vaporization rate of
 568 6.4 mg/min was obtained. With a decrease of the flow rate to 2.5 NL/min and the same gaseous
 569 composition [12], the vaporization rate was of 3.2 mg/min. In START tests [3], it was
 570 demonstrated that the Ru vaporization rate, due to a much smaller interface area of the RuO₂
 571 crucible, is lower, close to 1.8 mg Ru/min. Higher Ru vaporization rate may favor the Ru
 572 aerosol formation in the tube.

573 The tube in VTT device was longer with an exit temperature lower than in START2. The
 574 fluid temperature at the outlet tube (location of gaseous and particles samples) is sampling at
 575 40 °C for VTT (tube exit) and at 410 °C for IRSN with a thermal gradient into the dipping tube
 576 of the first liquid trap cooled. This point influences the Ru speciation (gas/particle partition and
 577 deposition). IRSN sampling at 410 °C (tube exit) can be favorable to a higher gaseous fraction
 578 in the sample (RuO₄ and RuO₃) and favor the deposits in DT (RuO₂).

579 The reactivity at the surfaces could also influence the formation and transport of Ru
580 aerosols. It is worth noticing that the nature of the tube may change the results on account of
581 the reactions at the tube surface with pre-oxidized SS versus quartz. The Ru aerosols formation
582 and transport only exists with SS tube compared with quartz material in START experiments
583 [3]. In VTT the TGT is first an alumina tube in the high temperature furnace zone (1200° to
584 about 650°C) and next a pure SS tube (650°C to the exit of the tube) without pre-oxidized
585 treatment. Authors observed that the transport of RuO₄(g) was promoted by alumina tube rather
586 SS tube. So, the pre-oxidized treatment of SS tube has been done during the test with short
587 duration (< 60 min).

588 The experiments are consistent on the global Ru amount transported at the TGT outlet but
589 with a different gaseous and aerosol partition. In VTT tests, gaseous RuO₃-RuO₄ may form
590 RuO₂ particles between 410 °C and 40 °C as RuO₂ is much more thermochemically stable than
591 RuO₃.

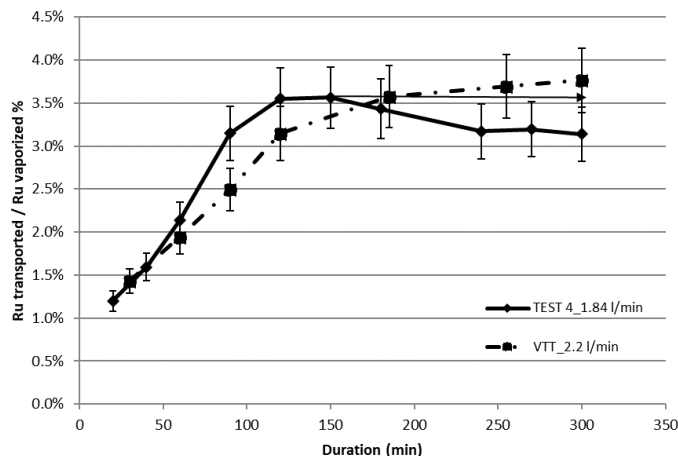
592 About the NO₂ influence, in VTT experiments, NO₂ was fed at 1227 °C and it resulted in
593 the decomposition of NO₂ to NO and O allowing possible oxidation of RuO₃ to RuO₄. Another
594 assumption is that NO₂ enhance RuO₄ existence at low temperatures, below 410 °C, preventing
595 RuO₃ decomposition into RuO₂. In our test conditions (sampling at 410°C), the influence of
596 NO₂ was not observed.

597 To get further, VTT and IRSN decided to make an experimental benchmark (Kärkelä T.,
598 OECD/NEA STEM2 Joint Project Meeting, personal communication, 2018, 27th June,
599 Boulogne-Billancourt France) with quite common conditions: a flow rate of 2.2 NL/min and
600 duration of 5h, changing of soda liquid traps every 30 to 70 minutes (7 samplings), NO₂ feed of
601 50 ppm in air saturated with water (20°C), a RuO₂ source of 200 mg with a crucible heated at
602 1227 °C (area: 8 cm x 2 cm). The main difference is the thermal gradient with the outlet
603 temperature much higher in IRSN device. Aerosol on-line measurements were performed with
604 combination of a differential mobility analyzer (DMA, particle size: 2 nm to 1 µm) and a
605 condensation particle counter (CPC, particles number) [12]. With a Ru vaporization rate
606 estimated at (3.0 ± 0.4) mg/min, the duration to consume all the reagent was about 55 min. The
607 Ru amount transported at the outlet at 40 °C (Fig. 11) was 3.8% i.i RuO₄(g), very similar to the
608 IRSN test 4 results (~3.5% i.i. at 150 min with outlet at 240 °C). Both results are consistent. No
609 aerosols were transported to the filter after 60 minutes of sampling (confirmed by on-line
610 measurements), contrary to previous experiments with 5 l/min (1.8 - 2.6 mg Ru metal). Possibly
611 NO₂ oxidized all RuO₃ into RuO₄. Therefore, RuO₂ formation was decreased. Some black
612 deposits inside the dipping tube of the soda trap were also observed as in START tests. As VTT
613 results are similar to START2 one (test 4), we can conclude that with « lower » flow rate (~2
614 l/min) no noticeable effect of NO₂ on RuO₄ transport at the outlet tube was observed whatever
615 the experimental device used. It can tend to suspect high influence of Ru flow inlet on
616 nucleation processes.

617 The measurement bias observed in START2, resulting from reactivity between dissolved
618 Ru and NO₂ in alkaline soda solution (evolution of the gaseous/aerosol partition in the first
619 trapping solution during the test and some black deposits on the glass wall observed at the end
620 of the test), was not observed in VTT test with the changing of liquid traps each 30 min. The
621 NO₂ dissolved in alkaline solution forms nitrite and nitrate ions which may later react to form
622 some ruthenium nitrosyl complexes with a certain kinetics. This observation confirms that there

623 was a formation of chemical reaction products in the first liquid trap in IRSN test 4 (perhaps,
624 nitrosyl ruthenium complex).

625



626

627 Fig. 11 Evolution of the Ru amount in the first liquid trap during the VTT and START2 tests

628

629 **CONCLUSIONS**

630 START2 experiments have investigated the ruthenium behavior along the RCS with oxidative
631 conditions. This point was identified as a main source of uncertainties to better evaluate
632 ruthenium source term. During a nuclear accident, the vaporization phase is a short-term
633 phenomenon while the revaporization phase should be a potential long continuous phase. So,
634 revaporization from the Ru deposit in the RCS must be considered to calculate the ruthenium
635 source terms as it is the most impacting due to delayed releases.

636 For reminder, the STEM project has shown that the Ru amount transported, under a gaseous
637 form, up to the tube outlet can reach about 4% of initial inventory. The Ru releases come from
638 about a similar contribution of the direct vaporization phase from the crucible (direct phase)
639 complemented by a revaporization phase from the Ru deposits (delayed releases). This 4%
640 cannot be considered as a conservative value because nuclear accident conditions are much
641 more complex than our test conditions and revaporization phase was not achieved.

642 The START2 ruthenium results allowed gaining knowledge on the key parameters
643 impacting the transport kinetics, the partition between gaseous and aerosols at the outlet of the
644 TGT and the extent of the revaporization process of deposited species. The experiments were
645 performed at 1200°C, with an abrupt profile and a pre-oxidized Stainless-Steel tube to be more
646 representative. The impact of the steam amount in carrier gas, the flow rate and NO₂/N₂O feed
647 (50 ppm) was studied.

648 The experimental data on Ru transport in the RCS support these conclusions:

- 649 - The long duration tests (7 hours) have evidenced the existence of transient phenomena
650 during the first hour (vaporisation phase), confirming the necessity to study the
651 ruthenium chemistry for several hours to catch the precise phenomenology.

- 652 - The Ru vaporization kinetics from the crucible (anhydrous RuO₂) in the furnace at
653 1200°C was characterized, with a good reproducibility, for different carrier gas mixtures
654 (H₂O/air) and was linearly steam mixture dependent. The dry air condition was the most
655 favorable condition for Ru vaporization. At a given temperature, Ru vaporization rate
656 from the crucible depended on the crucible geometry, the flow rate and the gaseous
657 composition of carrier gas (O₂ %).
- 658 - Whatever the gaseous composition (mixture of H₂O/air), most of the vaporized Ru was
659 deposited in the transport tube (> 80% of the released initial inventory i.i.).
- 660 - The higher the air amount in the carrier gas is, the higher the total Ru amount transported
661 at the outlet is, whatever the flow rate tested.
- 662 - For the tests performed with steam/air mixture and a flow rate of 1.84 NL/min during
663 7h, the Ru gaseous fraction at the outlet remains below to 3-4 % of the Ru mass
664 vaporized (i.i.) whatever the steam fraction (with Ru vaporization rate lower than
665 1.5 mg/min).
- 666 - The effect of flow rate is important: with a flow rate of 4.65 NL/min (factor x 2.5
667 compared to “standard” conditions of 1.84 NL/min), Ru gaseous fraction at the outlet
668 increased but remained below to 10% i.i. with excess of steam (SA condition).
- 669 - The Ru gaseous fraction comes from a direct transport (vaporization) and longer
670 revaporization from the Ru deposits (for T > 900 °C). With a higher flow rate, the
671 revaporization phase is less efficient and shorter, due to lower deposit build-up in the
672 TGT tube during the vaporization phase, leading to smaller formation of gaseous
673 ruthenium on the long term.
- 674 - Nitrogen oxides (NO₂ or N₂O feed, 50 ppm) do not increase the outlet gaseous Ru
675 fraction with our thermal-hydraulic conditions (T > 400°C). Indeed, NO/NO₂/N₂O
676 measurements at the outlet have shown a total decomposition of NO_x with a furnace
677 temperature at 1200°C and a flow rate lower than 5 NL/min.
- 678 - The Ru gaseous fraction at the tube outlet (~410 °C with 4.65 NL/min and ~290 °C with
679 1.84 NL/min) could be part of RuO₃ (consistent with remobilization of high temperature
680 deposits and thermal decomposition of RuO₄) which may be converted into RuO₄,
681 sampling at lower temperature in liquid traps.

682 At the end of this experimental study on Ru transport, some recommendations for Source Term
683 applications can be suggested:

- 684 i) There is a good representativeness of START device concerning the gas
685 composition (RuO_{3(g)} and RuO_{4(g)} species) and surface effects (pre-oxidized SS).
686 But, the higher surface/volume ratio in START device favors the surface effect (Ru
687 deposits amount). So, that trend tends to increase the gaseous fraction in the
688 Pressurised Water Reactor case. In return, the presence of aerosols inside the RCS
689 tends to decrease the gaseous fraction at the tube outlet due to sites of heterogeneous
690 nucleation. Data obtained are consistent with the transport of gaseous RuO₃.
- 691 ii) If we attribute the persistence of gaseous ruthenium during the direct phase to
692 persistence of RuO_{3(g)}, the increase of flow rate decreased the decomposition extent
693 due to kinetic limitation. For future models, it should be needed to consider a kinetic

694 of decomposition of RuO_{3(g)} into RuO₂ in bulk phase and, also on steel oxidized
695 surface. So, severe accident modelling should consider kinetics concerning the
696 conversion of RuO₃ into RuO₄ and non-congruent condensation processes.

697
698 START experimental data allow a better understanding of Ru transport inside the RCS with
699 oxidizing conditions. They also provide guidelines to develop/validate the models and
700 constitute a validation database for SA modelling. These experimental results are used to
701 improve the models currently implemented in the ASTEC IRSN software package (Accident
702 Source Term Evaluation Code) [19] and to reassess ruthenium source term in considering
703 potential gaseous ruthenium outside releases because current Ru ST only consider aerosol
704 releases. Depending on the level of confidence of the models of Ru behaviour in SA simulations
705 software for air-ingress scenarios, these reassessments will be performed either on modelling
706 simulations or based on quite reasonable conservatism approaches. The last step should be to
707 update PSA2 studies and according to potential radiological consequences try to define mitigate
708 means for the involved category of severe accident.

709
710

711 **Acknowledgments**

712 The authors acknowledge the OECD/NEA/CSNI hosting the STEM2 project and the STEM
713 project partners: Electricité De France, Canadian National Laboratories (Canada), VTT
714 Technical Research Centre of Finland Ltd (Finland), Nuclear Research Institute (Czech
715 Republic), Gesellschaft für Anlagen - und Reaktorsicherheit (Germany), Korea Atomic Energy
716 Research Institute, Korea Institute for Nuclear Safety, Nuclear Regulatory Commission (USA),
717 Swedish Radiation Safety Authority, National Nuclear Laboratory (England), Japan Atomic
718 Energy Agency and Nuclear Regulation Authority (Japan).

719 The authors also thank the CNRS Villeurbanne (CREALINS) for the measurements of Ru
720 deposit with the alkaline fusion method (L. Ayouni), K. Boucault, C. Gomez and S. Souvi from
721 IRSN for their technical contribution and fruitful discussion.

722
723 **Conflict of interest statement**

- 724 • The authors have no relevant financial or non-financial interests to disclose.
- 725 • The authors have no competing interests to declare that are relevant to the content of
726 this article.
- 727 • All authors certify that they have no affiliations with or involvement in any organization
728 or entity with any financial interest or non-financial interest in the subject matter or materials
729 discussed in this manuscript.
- 730 • The authors have no financial or proprietary interests in any material discussed in this
731 article.

732
733
734
735
736
737

738 List of abbreviations

739

Abbreviation	Definition
SA	Severe accident
NPP	Nuclear power plant
STEM	Source Term Evaluation and Mitigation
START	Study of the TrAnsport of RuThenium in the primary circuit
RCS	Reactor cooling system
PWR	Pressurized water reactor
TGT	Thermal gradient tube
SS	Stainless steel
DT	Dipping tube
DMA	Differential mobility analyzer
CPC	Condensation particle counter
ASTEC	Accident Source Term Evaluation Code

740

741

742

743 **References**

- 744 1. Miradji, F., F. Cousin, S. Souvi, V. Vallet, J. Denis, V. Tanchoux, and L. Cantrel. *Modelling*
745 *of Ru behaviour in oxidative accident conditions and first source term assessments*. in *The*
746 *7th European Review Meeting on Severe Accident Research (ERMSAR)*. 24-26 March 2015.
747 Marseille, France.
- 748 2. *START Ruthenium tests are part of the OECD/NEA Source Term Evaluation and Mitigation*
749 *(STEM) project*. <https://oecd-nea.org/jointproj/stem.html>.
- 750 3. Ohnet, M.N., O. Leroy, and A.S. Mamede, *Ruthenium behavior in the reactor cooling*
751 *system in case of a PWR severe accident*. *Journal of Radioanalytical and Nuclear Chemistry*,
752 2018. **316**(1): p. 161-177. DOI: 10.1007/s10967-018-5743-2.
- 753 4. Mun, C., L. Bosland, L. Cantrel, J. Colombani, O. Leroy, M.N. Ohnet, and T. Albiol. *OECD*
754 *STEM Project and its Follow-up STEM2*. in *International Iodine Workshop - Full*
755 *proceeding*. May 2016 2015. Marseille (France).
- 756 5. Cotton, F.A. and G. Wilkinson, *Advanced Inorganic Chemistry - A comprehensive Text*.
757 fourth ed, ed. J.W. Sons 1980.
- 758 6. Fletcher, J.M., I.L. Jenkins, F.M. Lever, F.S. Martin, A.R. Powell, and R. Todd, *Nitrato and*
759 *nitro complexes of nitrosylruthenium*. *Journal of Inorganic and Nuclear Chemistry*, 1955.
760 **1**(6): p. 378-401. DOI: 10.1016/0022-1902(55)80048-6.
- 761 7. Nerisson, P., M. Barrachin, M.N. Ohnet, and L. Cantrel, *Behaviour of ruthenium in nitric*
762 *media (HLLW) in reprocessing plants: a review and some perspectives*. *Journal of*
763 *Radioanalytical and Nuclear Chemistry*, 2022. **331**(9): p. 3365-3389. DOI: 10.1007/s10967-
764 022-08420-z.
- 765 8. Igarashi, H., K. Kato, and T. Takahashi, *Absorption Behaviour of Gaseous Ruthenium into*
766 *Water*. *Radiochimica Acta*, 1992. **57**(1): p. 51-55. DOI: 10.1524/ract.1992.57.1.51.
- 767 9. Mun, C., L. Cantrel, and C. Madic, *Review of literature on ruthenium behavior in nuclear*
768 *power plant severe accidents*. *Nuclear Technology*, 2006. **156**(3): p. 332-346.
- 769 10. Bosland, L., F. Funke, N. Girault, and G. Langrock, *PARIS project: Radiolytic oxidation of*
770 *molecular iodine in containment during a nuclear reactor severe accident: Part I.*
771 *Formation and destruction of air radiolysis products—Experimental results and modelling*.
772 *Nuclear Engineering and Design*, 2008. **238**(12): p. 3542-3550. DOI:
773 <https://doi.org/10.1016/j.nucengdes.2008.06.023>.
- 774 11. Mamede, A.S., N. Nuns, A.L. Cristol, L. Cantrel, S. Souvi, S. Cristol, and J.F. Paul,
775 *Multitechnique characterisation of 304L surface states oxidised at high temperature in*
776 *steam and air atmospheres*. *Applied Surface Science*, 2016. **369**: p. 510-519. DOI:
777 10.1016/j.apsusc.2016.01.185.
- 778 12. Kajan, I., T. Kärkelä, A. Auvinen, and C. Ekberg, *Effect of nitrogen compounds on*
779 *transport of ruthenium through the RCS*. *Journal of Radioanalytical and Nuclear Chemistry*,
780 2017. **311**(3): p. 2097-2109. DOI: 10.1007/s10967-017-5172-7.
- 781 13. Kajan, I., T. Kärkelä, U. Tapper, L.S. Johansson, M. Gouëlle, H. Ramebäck, S. Holmgren,
782 A. Auvinen, and C. Ekberg, *Impact of Ag and NOx compounds on the transport of*
783 *ruthenium in the primary circuit of nuclear power plant in a severe accident*. *Annals of*
784 *Nuclear Energy*, 2017. **100**: p. 9-19. DOI: 10.1016/j.anucene.2016.10.008.
- 785 14. Kärkelä, T., U. Backman, A. Auvinen, R. Zilliacus, M. Lipponen, T. Kekki, U. Tapper, and
786 J. Jokiniemi, *Experiments on the behaviour of ruthenium in air ingress accidents - Final*
787 *report*, in *SARNET-ST-P58 2007*, VTT Processes: Espoo - Finland.
- 788 15. Klein, M., C. Weyers, and W.R.A. Goossens. *Volatilization and trapping of ruthenium in*
789 *high temperature processes in Proceedings of the 17th DOE Nuclear Air Cleaning*
790 *Conference*. August 1982.

- 791 16. Briner, E., C. Meiner, and A. Rothen, *La décomposition du protoxyde d'azote aux*
792 *températures élevées*. Helvetica Chimica Acta, 1926. **9**(1): p. 409-141.DOI:
793 10.1002/hlca.19260090150.
- 794 17. Miradji, F. Quantum Modelling of Ruthenium Chemistry in the field of Nuclear Power Plant
795 Safety 2016. University of Lille <http://www.theses.fr/2016LIL10192>
- 796 18. Miradji, F., S.M.O. Souvi, L. Cantrel, F. Louis, and V. Vallet, *Reactivity of Ru oxides with*
797 *air radiolysis products investigated by theoretical calculations*. Journal of Nuclear
798 Materials, 2022. **558**.DOI: 10.1016/j.jnucmat.2021.153395.
- 799 19. Chatelard, P., S. Belon, L. Bosland, L. Carénini, O. Coindreau, F. Cousin, C. Marchetto, H.
800 Nowack, L. Piar, and L. Chailan, *Main modelling features of the ASTEC V2.1 major*
801 *version*. Annals of Nuclear Energy, 2016. **93**: p. 83-93.DOI:
802 10.1016/j.anucene.2015.12.026.
- 803
- 804